Tan, C. M., Chin, C. M., Sim, M. L., & Beach, M. A. (2006). Modelling the general dependency between directions of arrival and departure for an indoor MIMO channel. IEEE Vehicular Technology Conference, 6, 2878 - 2882. 10.1109/VETECS.2006.1683394

Modelling the General Dependency Between Directions of Arrival and Departure for an Indoor MIMO Channel

C. M. Tan[1], C. M. Chin[1], M. L. Sim[1], and M. A. Beach[2]

[1]British Telecom Asian Research Centre,
63000 Selangor, Malaysia.
email: {chormin.tan, eric.chin, mohlim.sim}@bt.com

[2]Centre for Communications Research,
University of Bristol, UK.
email: m.a.beach@bristol.ac.uk

Abstract— **Precise modelling of the Direction of Arrival (DoA) and Direction of Departure (DoD) of multipath components (MPCs) in a Multiple-Input Multiple-Output (MIMO) channel based on correlation properties and joint distributions have not been investigated properly. This paper examines the correlation between DoAs and DoDs, and presents a modelling approach particularly for the '*general trend*' of these dual-spatial domains, based on statistical results obtained from several indoor MIMO measurement campaigns. We show that the Laplacian distribution provides better fits for the directional parameters than the normal and Von Mises distributions. The '*general trend*' of DoA/DoD joint distribution and power density are modelled using a *modified Gumbel's bivariate exponential* approach. Results show that the proposed bivariate distribution provides a good match to the real data, and offers an alternative approach to generate realistic directional-based stochastic MIMO channel responses in different environments.**

I. Introduction

MIMO technologies have now emerged as one of the most promising approaches to increase channel capacity and data rate without expansion in bandwidth and transmit power. Many wireless systems have also incorporated MIMO technologies into their standards, e.g. IEEE 802.11n (in progress), 802.16, and 3GPP/3GPP2. In order to assess the performance of MIMO systems, realistic models of the channels are required. These models must be able to reproduce accurate correlation properties of the channel propagation mechanisms as viewed from both transmitter (Tx) and receiver (Rx).

Many MIMO channel models have been proposed in recent years (via measurement campaigns), where excellent discussions and reviews of different modelling approaches can be found in European COST 273 [1] and NEWCOM [2] projects. Amongst the various modelling approaches, physical model (e.g. geometrical based stochastic modelling) has received considerable attentions especially in COST 273 [1]. It is able to generate realistic MIMO channel responses based on the propagation mechanisms of different wireless environments. Unlike the non-physical models such as the Weichselberger and Kronecker models, physical models are independent of antenna characteristics and responses of measurement equipment, as only the double-directional propagation channel [3] is modelled. This requires accurate DoA and DoD information of the MPCs, and the ability to isolate responses of antennas from the measured channel in offline processing.

Previous measurement results have resolved the debates regarding the inter-relationship of DoAs and DoDs. It has been confirmed that certain degrees of dependency occur between DoAs and DoDs [4][5], and hence the statistics of both parameters are non-separable [6] and must be described properly by their joint distribution functions as applied to different types of environments (e.g. office, corridor, open area, etc). Despite considerable number of investigations in this particular area, to the best knowledge of the authors, nobody has ever modelled the joint distributions of DoAs and DoDs through real observation of measurement results. This is especially so when considering their joint distributions around the full azimuth plane at both sides, taking into account of their correlations.

This paper describes a modelling approach for the joint distributions of DoA and DoD components, as well as their joint power density. Primarily, the model considers the '*general trend*' observed in these domains, which is similar in many environments that have been investigated [4][5]. The so-called '*trend*' shows that most MPCs tend to concentrate around the directional regions where both Tx and Rx face each other, and both DoAs and DoDs are not evenly distributed around the azimuth. Here, our goodness of fit analysis reveals that the global distributions of both parameters are close to Laplacian but not normally distributed. In terms of double-directional modelling, we propose a '2-D Laplacian-like', or *modified Gumbel's bivariate exponential* joint distribution to model the MPCs and power density in the dual-spatial domains, where a good match to the real data can be achieved. The paper begins with a brief description of the channel sounding procedure, indoor environments, and parameter extraction process. The main focus of the paper is dedicated to the discussions of the double-directional modelling framework for the '*general trend*' observed in these indoor environments.

II. Measurement Procedure and Environments

Several extensive dynamic wideband double-directional/ MIMO measurement campaigns were conducted using the Medav RUSK BRI channel sounder, with advanced techniques capable of providing high-resolution supports [7], thus increasing the efficiency in channel sounding and easing the data processing procedure. A novel feature of the measurement was its ability to provide instantaneous full azimuth views at both ends by employing a pair of 16-element uniform circular patch arrays (UCPAs) [8]. Although the arrays were dual-polarised, only vertical polarisation was considered throughout

0-7803-9392-9/06/$20.00 (c) 2006 IEEE

the measurements. Two additional array switching units were constructed as an external interface between the UCPAs and the sounder core units. These additional units ensured synchronised MIMO sequential switching sequence at both transmitting and receiving arrays. Back-to-back calibration procedure was performed prior to all measurements in order to remove hardware responses from the measured channels. Also, spatial calibration process was performed in an anechoic chamber prior to the measurement campaigns in order to capture the actual array manifold in 0.5° angular steps over the full azimuth range.

The sounding bandwidth was set to 120 MHz (centred at 5.2 GHz), and the period of the transmitted multitone signal was 0.8 µs. The height (measured from centroid of patch elements) of Rx was fixed at 1.7 m from ground at all times, while the height of Tx was fixed at either 1.7 m for peer-to-peer measurements, or 3 m to emulate an access point. Dynamic measurements were conducted such that the Tx was fixed at a specific location, while the Rx was slowly pushed (≈ 0.2 m/s) along a convenient path with a customised trolley. While the Rx was being pushed, 1 MIMO snapshot (16×16) was recorded every 15.36 ms. For more detailed descriptions of the measurements and other supplementary considerations, interested reader is referred to [8].

The measurements were conducted in 4 different indoor environments typical for wireless network deployments: office, corridor, open foyer, and laboratory. The environments were highly cluttered (most cases), with standard furniture (wooden shelves, metal cabinets, tables, soft-boards, etc.) throughout. There was no restriction imposed on the environments, as people were allowed to move around freely (to emulate real wireless scenario). Different propagation conditions were considered: populated, unpopulated, line of sight (LOS), obstructed or non-LOS (OLOS/NLOS), etc. In order to ease the following discussions, a sample floor plan in a large office environment is shown in Fig. 1. The fixed positions for each Tx (only one active at any time), the dynamic path of the Rx, and also the 0° reference of the UCPA, are all self-explained in the floor plan. Due to space limitation, interested reader is referred to [4] and [5] for additional descriptions, floor plans, and pictures of all the measured indoor environments.

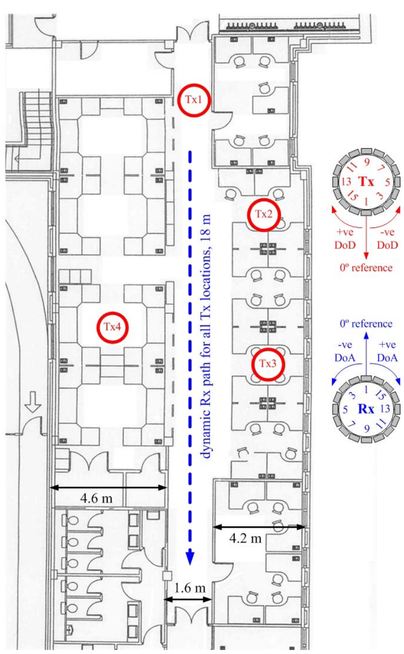

Figure 1: Floor plan of a large office environment

III. MULTIPATH PARAMETER EXTRACTION

In order to develop stochastic physical channel models, the multipath parameters, such as the time delay of arrival (TDoA), DoD, DoA, and Doppler shift, must be extracted from the measurement raw data. This process is usually accomplished with the aids of high-resolution multi-dimensional estimation algorithms (good review in [9]). Results of investigations given in [10] reveal that the Space Alternating Generalised Expectation-maximisation (SAGE) algorithm [11] offers the best performance when applied to circular array(s). In order to further reduce the overall processing time, the Hybrid-Space SAGE (HS-SAGE) algorithm has been proposed [12]. The HS-SAGE algorithm extracts the multi-dimensional parameter in a combination of element-space and beamspace domains. In beamspace processing, a number of beams are formed across the subset of the entire supportable estimation space (certain conditions applied). Iterative estimation processes are only executed across this subset of beamspace of reduced dimensionality in terms of input data size, thus a reduction in overall computation time.

Here, the 3-D HS-SAGE algorithm [12] was employed to extract the TDoA, DoA, DoD, and path gain of the MPCs from raw data collected in these measurement campaigns. Both DoAs and DoDs are estimated in the normal element-space domain, while the TDoAs are estimated in the beamspace domain. Beamspace processing was focused in 0-400 ns temporal region as it was observed that (almost) all MPCs concentrated in this region within the 30 dB power window (from the strongest path). Each set of results was estimated from 5 consecutive MIMO snapshots along the dynamic path. With more than 15 Gbytes of compressed raw database, the extracted 3-D multipath parameter data can be used to represent meaningful and realistic statistics as observed in a real MIMO environment.

IV. DOUBLE-DIRECTIONAL MODELLING

The main analysis in this paper is only focused on DoA (ϕ_{RX}) and DoD (ϕ_{TX}) azimuth domains, albeit the support of TDoA extraction from the 3-D HS-SAGE algorithm. Also, the paper considers only the modelling framework for the '*general trend*' of the DoAs and DoDs as commonly observed in the joint distributions in different measurement locations and environments. The proposed framework provides alternative means to generate MIMO channel responses based on 'double-directional' approach [3], and is generic to all environments and propagation conditions. Additional features of the channel (e.g. clustering phenomena, dynamic evolutions of MPCs, TDoA distributions, etc) can be easily included as an overlay of the framework, such that special propagation conditions (e.g. far scatterers, number of clusters) can be customised according to the specific behaviour of the environments.

As the measurements were conducted in dynamic mode, the directional parameters associated to a particular MPC would change as a function of mobile Rx displacement along the dynamic route. In order to gain a better insight into the overall dependency between the directional parameters, the UCPA orientations were artificially readjusted in offline processing such that both UCPAs faced each other at their respective normalised 0° reference axis throughout the whole dynamic path. This directional normalisation procedure was performed manually by visual inspection, based on the knowledge of estimated multipath parameters[1], as well as the geometrical structure of the environments (to the best accuracy). Hence, the observed distribution effectively represents instantaneous distribution of the MPCs, for any realisation of the MIMO channel in environments of similar nature.

Fig. 2 presents a sample of the DoA-DoD joint distribution for results corresponding to measurements conducted at 'Tx1' location (1.7 m) in an office environment (Fig. 1). For other joint distributions in other office locations or indoor environments, interested reader is referred to [4] and [5]. Accordingly, the joint distributions have a '*general trend*' showing that considerable amount of MPCs tend to concentrate around the directional regions aligned to the axis where both terminals faced each other, as well as regions in which either one faced the opposite direction.

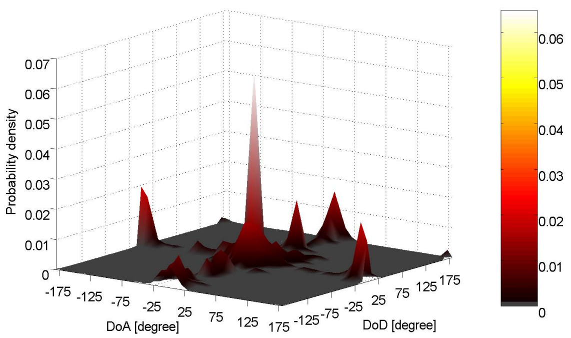

Figure 2: DoA and DoD joint distribution for 'Tx1' measurements in an office environment (LOS)[2]

In summary, there are 3 regions where significant concentration of MPCs can be found (see Fig. 3):

- Region A: $\phi_{TX}\in[-50°,50°]$, $\phi_{RX}\in[-50°,50°]$,
- Region B: $\phi_{TX}\in[-50°,50°]$, $\phi_{RX}\in[-180°,-130°]\cup[130°, 180°]$,
- Region C: $\phi_{TX}\in[-180°,-130°]\cup[130°, 180°]$, $\phi_{RX}\in[-50°,50°]$.

Here, 0° (at both Tx and Rx) is the reference direction where both terminals faced each other. All the extracted DoAs and DoDs corresponding to all measurements are normalised to this reference. Also, the angular location of -180° is physically equivalent to 180°.

[1] It was observed that in most cases, including in a complete NLOS condition, the DoA of the strongest path was always facing the angular location of the Tx, and vice-versa for the DoD.

[2] Directional normalisation procedure was not performed for 'Tx1' measurement in the office environment, as the 0° UCPA orientation for both Tx and Rx was facing each other throughout the dynamic route.

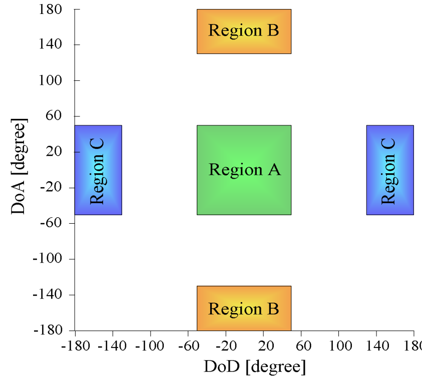

Figure 3: The '*general trend*' of DoA (ϕ_{RX}) and DoD (ϕ_{TX}) concentration

The most common spatial distributions under regular studies and debates are the normal, Laplacian, and Von Mises distributions. Fig 4 presents several distribution fits for DoAs in 'Region A' (of that in Fig. 2). Our analysis reveals that the directional parameter is close to Laplacian (double exponential) distributed. This observation is based on the resolution supported by the measurement equipment and the multi-dimensional estimation algorithm (3-D HS-SAGE). From simulation results, the averaged spatial and temporal resolution (for this particular measurement setting) is ~10° and ~4 ns respectively, which is much higher than the intrinsic Rayleigh resolution of ~22° and ~8 ns. This is considered sufficient and good enough to represent the propagation channel as seen by most wireless devices in any real indoor environments.

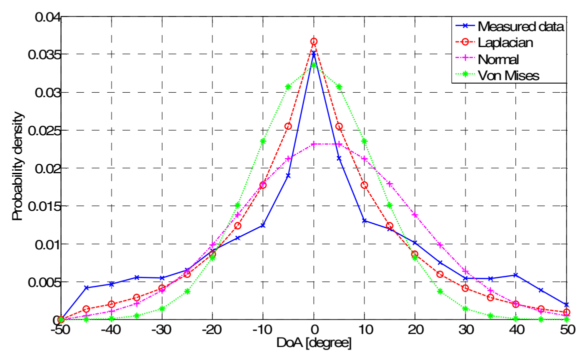

Figure 4: Fitted probability densities of DoA in 'Region A' in the office

In addition, the joint distribution of DoA and DoD in Regions A-C also exhibit Laplacian characteristics when viewed from their respective domains. This phenomenon is observed visually from the joint distributions (e.g. Fig. 2). Hence, the model for the joint distributions should also exhibit Laplacian characteristics in the dual-spatial domain, which can be achieved using a *2-D Laplacian*-like approach, or the bivariate exponential approach. Several bivariate exponential distributions have been derived [13], e.g. Arnold and Strauss', Hougaard's, Downton's, Gumbel's, Freund's, Marshall and Olkin's, etc. These bivariate exponential functions are able to provide a good fit to the observed data, which also consider the correlation properties between the 2 random data domains. However, most functions involve a number of variables and sub-expressions, which have directly increased the numerical complexity and computational burden of the model. Some expressions also involve complicated routines that are sometimes difficult to accomplish while preserving accuracy.

It should be noted that the development of a model must be made simple with elegant formulation, and yet able to preserve as many important properties and characteristics of the channel as possible, and with minimum compensation in terms of accuracy and reliability. Hence, we propose a *modified Gumbel's bivariate exponential expression* for modeling the DoA-DoD joint distribution:

$$f(\phi_{\mathrm{TX}},\phi_{\mathrm{RX}}) = \mathrm{K}\ \exp\left(-\left|\frac{|\phi_{\mathrm{TX}}|-\mu_{\mathrm{TX}}}{\sigma_{\mathrm{TX}}}\right| - \left|\frac{|\phi_{\mathrm{RX}}|-\mu_{\mathrm{RX}}}{\sigma_{\mathrm{RX}}}\right| - \gamma\left|\frac{|\phi_{\mathrm{TX}}|-\mu_{\mathrm{TX}}}{\sigma_{\mathrm{TX}}}\right|\left|\frac{|\phi_{\mathrm{RX}}|-\mu_{\mathrm{RX}}}{\sigma_{\mathrm{RX}}}\right| \right) \quad (1),$$

where $(\sigma_{\mathrm{TX}},\sigma_{\mathrm{RX}})$ denotes the DoD/DoA angular spread, $(\mu_{\mathrm{TX}},\mu_{\mathrm{RX}})$ is the mean of DoD/DoA, K is a scaling factor so that the overall volume ($\phi_{\mathrm{TX}}\in$[-180°,180°], $\phi_{\mathrm{RX}}\in$[-180°,180°]) of the resultant joint distribution equals to 1, and $\gamma\in[0,1]$ is related to the correlation coefficient (ρ), given by:

$$\rho = -1 - \frac{1}{\gamma}\exp(1/\gamma)\,\mathrm{E_i}(-1/\gamma) \quad (2),$$

and $\mathrm{E_i}(\cdot)$ is the exponential integral function defined by:

$$\mathrm{E_i}(x) = -\int_{-x}^{\infty}\frac{\exp(-y)}{y}dy \quad (3).$$

The above expressions are applied separately on different 'Regions', with different sets of σ, μ, γ and K. The variable 'K' determines the probability of the 2-D random numbers falling into a specific 'Region'. Equation (1) considers the correlation between DoA and DoD via the 'γ' expression. The procedure to generate the 2-D random numbers with correlation considerations can be found in [14] and [15].

In order to further reduce the complexity, the random number generation process across the DoA and DoD domains can be implemented separately in 1-D case as follows:

$$f(\phi_{\mathrm{TX}},\phi_{\mathrm{RX}}) = \mathrm{K}\ \exp\left(-\left|\frac{|\phi_{\mathrm{TX}}|-\mu_{\mathrm{TX}}}{\sigma_{\mathrm{TX}}}\right|\right)\exp\left(-\left|\frac{|\phi_{\mathrm{RX}}|-\mu_{\mathrm{RX}}}{\sigma_{\mathrm{RX}}}\right|\right) \quad (4).$$

However, this can only be done when both DoA and DoD are uncorrelated, or loosely correlated ($\rho \to 0$ then $\gamma \to 0$).

The calculated $|\rho|$ and K values in different environments are presented in Table 1, for measurements corresponding to Tx height at 1.7 m. It can be seen that ρ has a low value in most cases. However, ρ's for 'Office (OLOS/NLOS) Region B/C' and 'Open Foyer' are significantly higher. However, that does not necessarily imply that both DoA and DoD in these cases are highly correlated. It should be noted that the accuracy of ρ decreases and could be unreliable in case of large dataset, that even weak associations may be found to be statistically significant [16]. There is no recommended range of dataset for use in ρ computation, as the impact of different datasets on the accuracy of ρ is still an open area of research. For the results presented in Table 1, the ρ values are computed using all samples of DoAs and DoDs (>50,000 in most cases).

Table 1: Calculated values of $|\rho|$, K and percentage power (for Regions A-C)

Environment	Region	$\lvert\rho\rvert$	K	Power %
Office (LOS)	A	0.0209	0.4686	82.38
	B	0.0147	0.1188	1.67
	C	0.0594	0.1869	11.51
Office (OLOS/ NLOS)	A	0.0891	0.2770	60.20
	B	0.6005	0.1081	5.12
	C	0.5460	0.1309	6.61
Open Foyer (LOS/OLOS)	A	0.3726	0.3094	67.40
	B	0.3912	0.1087	3.58
	C	0.5670	0.1478	15.60
Corridor (LOS)	A	0.0184	0.4552	87.93
	B	0.1006	0.1559	3.56
	C	0.2592	0.1236	3.21

Figure 5 presents the joint distribution for DoA/DoD data generated based on the calculated parameter values (σ, μ, γ, K) in Regions A-C of an office environment (LOS). For this particular example, the 2-D data for all 3 Regions are generated using the function given in Eq. (4), since $\rho = O(10^{-2})$ and $\gamma \approx 0$. The respective σ and μ values are tabulated in Table 2. The real distribution (confined to Regions A-C) obtained from measurement result is also presented in Fig. 6, where it can be seen that the simulated distribution for the '*general trend*' of DoA and DoD matches well with that of the real distribution.

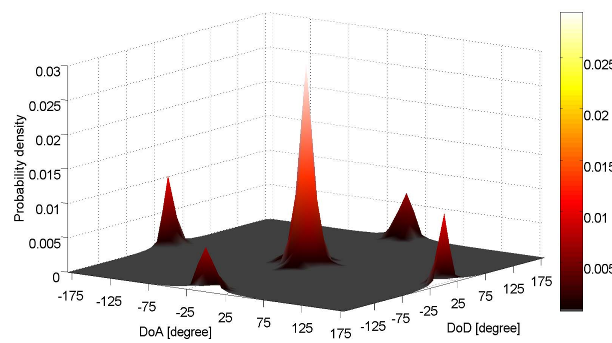

Figure 5: Joint density plot for the simulated DoA/DoD data in the office LOS environment (Regions A-C)

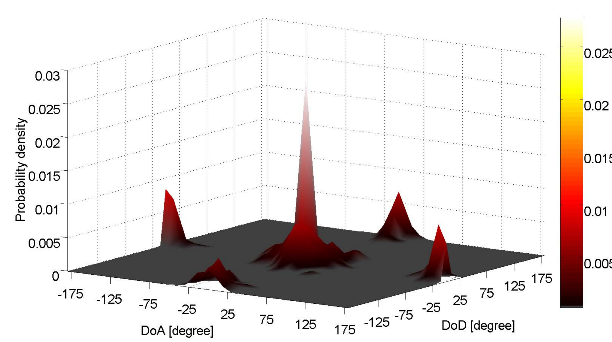

Figure 6: Joint density plot for the DoA/DoD data in the office LOS environment (Regions A-C) obtained from measurement results

Table 2: Regional parameters (in degrees) of modified Gumbel's bivariate exponential functions for the office environment (LOS)

Region	$f(\phi_{TX}, \phi_{RX})$			
	μ_{TX}	σ_{TX}	μ_{RX}	σ_{RX}
A	0	15.53	0	15.92
B	0	19.38	180	12.87
C	180	8.14	0	16.85

In addition, it was found that the power azimuth spectrum (PAS) at both the Tx and Rx also exhibited Laplacian-like characteristics [4][5], where majority of the strong components are concentrated in 'Region A' (see power percentage in Table 1). Hence, the same bivariate approach can be applied to model the joint power density. Similarly, in the case of weak association between both Tx and Rx, the expression for the joint power density can be simplified to:

$$\mathrm{P}(\phi_{TX}, \phi_{RX}) \propto \exp\left(-\left|\frac{|\phi_{TX}| - \hat{\mu}_{TX}}{\hat{\sigma}_{TX}}\right|\right) \exp\left(-\left|\frac{|\phi_{RX}| - \hat{\mu}_{RX}}{\hat{\sigma}_{RX}}\right|\right) \quad (5),$$

where $\hat{\sigma}_{TX}$ and $\hat{\sigma}_{RX}$ are respectively the 1st moment of the PAS at Tx and Rx, and $\hat{\mu}_{TX}$ and $\hat{\mu}_{RX}$ are the square root of 2nd central moment of the PAS at Tx and Rx, respectively.

Using the expression in Eq. 5, the simulated joint power density in 'Region A' of the same office LOS environment is presented in Fig. 7, where the result matches well with that from the measurements shown in Fig. 8. In this particular example, the parameters in Eq. 5 are determined using the square-root fitting approach, with values: $(\hat{\sigma}_{TX}, \hat{\sigma}_{RX}) = (9.0°, 11.7°)$, and $(\hat{\mu}_{TX}, \hat{\mu}_{RX}) = (0°, 0°)$.

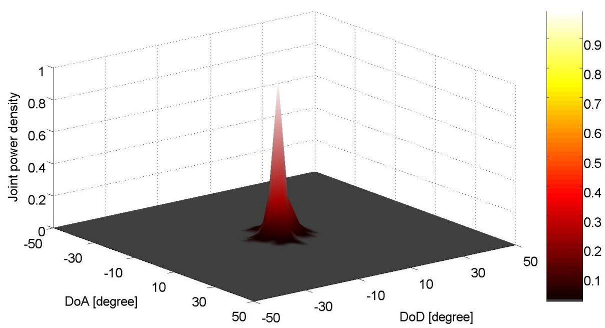

Figure 7: Joint power density plot at 'Region A' in the office LOS environment using the simulated results (the peak is normalised to 1)

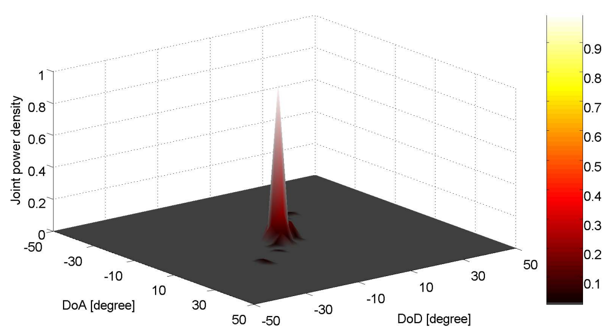

Figure 8: Joint power density plot at 'Region A' in the office LOS environment using the measurement results (the peak is normalised to 1)

V. Conclusions

A joint distribution modelling approach using the *modified Gumbel's bivariate exponential expression* for the '*general trend*' of the DoAs and DoDs is presented in this paper. It is shown that results from the proposed approach match well with that from the real measurement data. It should be noted that the main focus of this paper is to model the common '*trend*' (i.e. Regions A-C) as observed in several indoor environments. The approach is generic, and extra modelling procedure (e.g. clustering, birth-death phenomenon, delays, etc.) is needed in order to generate complete channel responses specific to various unique characteristics in different environments.

Acknowledgment

The measurement campaigns reported in this paper have been funded by the Virtual Centre of Excellence in Mobile and Personal Communications (http://www.mobilevce.com).

References

[1] European Cooperation in the field of Scientific and Technical Research – Action 273 (COST 273), http://www.lx.it.pt/cost273/.

[2] Network of Excellence in Wireless Communications (NEWCOM), http://newcom.ismb.it/public/index.jsp.

[3] M. Steinbauer, A. F. Molisch, and E. Bonek, "The double-directional radio channel," IEEE AP Magazine, vol. 43, no. 4, August 2001.

[4] C. M. Tan, M. A. Beach, and A. R. Nix, "Statistical characterization of double-directional channels in modern office environments," SPWC, London, UK, 2-4 June 2004.

[5] C. M. Tan, D. L. Paul, M. A. Beach, A. R. Nix, and C. J. Railton, "Dynamic double-directional propagation channel analysis with dual circular arrays," Joint European COST 273/284 Workshop, Gothenburg, Sweden, 7-10 June 2004.

[6] A. F. Molisch, "A generic model for MIMO wireless propagation channels in macro- and microcells," IEEE Trans Sig. Proc., vol. 52, no. 1, January 2005, pp. 61-71.

[7] R. S. Thomä, et al., "Identification of time-variant directional mobile radio channels," IEEE Trans. Instrum. and Meas., vol. 49, April 2000, pp. 357–364.

[8] M. A. Beach, C. M. Tan, and A. R. Nix, "Indoor dynamic double-directional measurements," ICEAA, Torino, Italy, 8-12 September 2003.

[9] H. Krim, and M. Viberg, "Two decades of array signal processing research," IEEE Sig. Proc. Mag., July 1996, pp. 67-94.

[10] C. M. Tan, P. Fletcher, M. A. Beach, A. R. Nix, M. Landmann, and R. S. Thomä, "On the application of circular arrays in direction finding, Part I: Investigation into the estimation algorithms," 1st European COST 273 Workshop, Espoo, Finland, 29-30 May 2002.

[11] B. H. Fleury, M. Tschudin, R. Heddergott, D. Dahlhaus, and K. I. Pedersen, "Channel parameter estimation in mobile radio environments using the SAGE algorithm," IEEE JSAC, vol. 17, March, pp. 434-450.

[12] C. M. Tan, M. A. Beach, and A. R. Nix, "Multidimensional hybrid-space SAGE algorithm: Joint element-space and beamspace processing," IST Mobile and Wireless Communications Summit 2003, Aveiro, Portugal, 15-18 June 2003.

[13] S. Nadarajah, and S. Kotz, "Reliability for some bivariate exponential distributions," Technical report, University of Nebraska, Lincoln, USA.

[14] B. C. Arnold and D. J. Strauss, "Bivariate distributions with conditionals in prescribed exponential families," J. Roy. Stat. Soc. Series B, vol. 53, 1991, pp. 365-375.

[15] M. E. Johnson, "Multivariate statistical simulation," John Wiley & Sons, New York, 1987.

[16] A. Agresti, "Categorical data analysis," John Wiley and Sons, New York, 1990.